HHS Public Access

Author manuscript

Dev Neurosci. Author manuscript; available in PMC 2015 November 14.

Published in final edited form as:

Dev Neurosci. 2015 November ; 37(6): 515–532. doi:10.1159/000438749.

Stereotaxic MRI brain atlases for infants from 3 to 12 months

Paul T. Fillmore[1], **John E. Richards**[2], **Michelle C. Phillips-Meek**[3], **Alison Cryer**[4], and **Michael Stevens**[2]

[1] Department of Communication Sciences and Disorders, University of South Carolina, Columbia, SC

[2] Department of Psychology and Institute for Mind and Brain, University of South Carolina, Columbia, SC

[3] Department of Psychology, University of South Carolina; Current affiliation: Department of Psychology, Limestone College.

[4] Department of Psychology, University of South Carolina

Abstract

Background—Accurate labeling of brain structures within an individual or group is a key issue in neuroimaging. Methods for labeling infant brains have depended on the labels done on adult brains or average MRI templates based on adult brains. However, the features of adult brains differ in several ways from infant brains, so the creation of a labeled stereotaxic atlas based on infants would be helpful. The current work builds on recent creation of age-appropriate average MRI templates during the first year (3, 4.5, 6, 7.5, 9, and 12 months), by creating anatomical label sets for each template.

Methods—We created stereotaxic atlases for the age-specific average MRI templates. Manual delineation of cortical and subcortical areas was done on the average templates based on infants during the first year. We also applied a procedure for automatic computation of macroanatomical atlases for individual infant participants using two manually segmented adult atlases (Hammers, LPBA40). To evaluate our methods, we did manual delineation of several cortical areas on selected individuals from each age. Linear and nonlinear registration of the individual and average template was used to transform the average atlas into the individual participant's space, and the average transformed atlas was compared to the individual manually delineated brain areas. We also applied these methods to an external dataset, not used in the atlas creation, to test generalizability of the atlases.

Results—Age-appropriate manual atlases were the best fit to the individual manually delineated regions, with more error seen at greater age discrepancy. There was a close fit between the manually delineated and the automatically labeled regions for individual participants, and for the age-appropriate template based atlas transformed into participant space. There was close correspondence between automatic labeling of individual brain regions, and those from the age-

Correspondence concerning this article should be addressed to: John E. Richards, Department of Psychology, University of South Carolina, Columbia, South Carolina, 29208; richards-john@sc.edu; phone: (803) 777-2079; fax: 803 777-9558..
Current affiliation: Department of Communication Sciences and Disorders, Baylor University, Waco, TX

appropriate template. Finally, these relationships held, even when tested on an external set of images.

Conclusion—We have created age-appropriate labeled templates for use in the study of infant development at 6 ages (3, 4.5, 6, 7.5, 9, and 12 months). Comparison with manual methods was quite good. We developed three stereotaxic atlases (one manual, two automatic) for each infant age, which should allow fine-grained analysis of brain structure for these populations than was previously possible with existing tools. The template-based atlases constructed in the current study are available online (http://jerlab.psych.sc.edu/NeurodevelopmentalMRIDatabase).

Keywords

atlas; MRI; neurodevelopment; infant

Magnetic resonance imaging (MRI) in infants allows for quantitative and qualitative assessment of neural development, which can enhance our understanding of early brain growth patterns and morphological changes during both normal and abnormal brain development. However, the quantitative study of infant brain development has been hampered by a lack of tools for structural analysis of the brain with MRI, in that tools which have been well validated in adults are often not validated for use with infants ([1]). For example, adult neuroimaging work generally uses average MRI templates and stereotaxic atlases to identify anatomical locations in the brain, but these adult stereotaxic atlases may not identify locations accurately in the developing brain. In the current work, we created a set of anatomically labeled stereotaxic atlases for infants from 3 to 12 months (3, 4.5, 6, 7.5, 9 and 12 months). These atlases should be more accurate for infant participants than atlases created with adult participants.

There have been four primary approaches to neuroanatomical labeling of brain structures in adults, summarized in Table 1. All of these approaches result in a stereotaxic atlas, generally represented in a MRI volume, which identifies anatomical areas. The validity of these approaches may be tested against a “gold standard” by manually delineating segmented regions in an individual participant, and comparing an atlas which has been registered to the participant's brain against the manual delineation. Creation of the LPBA40 atlas ([2]), for example, required manual delineation of regions on the 40 individuals from whom the atlas was derived. This method is time-consuming, typically requiring one or more individuals be trained on manual delineation protocols. In addition, the results from one individual are not easily transferable to new MRIs. The development of methods that could make use of pre-existing manual delineations would be highly desirable.

Studies of brain development in pediatric populations require similar atlases based on age-appropriate MRIs. One approach has been to register infant (or child, adolescent) brains to a labeled adult average template, and transform the adult atlas back into the space of the developing brain. Recent studies have shown that the use of adult reference data compromises the analysis of infant brain images ([3]; [4]; [5]; for review, see [1]). There are at least two stereotaxic atlases that have been created for infants in the first two years ([6]; [7]). Both of these atlases are based on registering infants to an atlas based on the manual

segmentation of the average MRI of one young adult (AAL; [8]), and may remain biased by that individual's specific anatomy.

The current study constructed manually delineated and automatically-derived anatomically-labeled stereotaxic atlases for infant ages. Our goals were to construct the automatic atlases and validate them against manually delineated individual participant atlases. Thus, our first objective was to create a manually labeled, age-specific stereotaxic atlas for average MRI templates for infants at 3, 4.5, 6, 7.5, 9, and 12 months of age on average MRI templates ([1]; [5];[9];[10]). We performed manual delineation of 14 areas (lobar and sub-lobar) on each infant-based age-specific template.

The second objective was to create automatically-labeled atlases for infants in the first year by adapting the procedures that Gousias and colleagues ([11]) used with 2-year-olds. We used the 30 adults from the Hammers adult brain atlas (83 manually delineated areas; Hammers atlases; [12];[13];[14]) and the 40 adults from the LONI Probabilistic Brain Atlas project (56 manually delineated areas; LPBA40; [2]), to create two macroanatomical atlases for individual infants at 3, 4.5, 6, 7.5, 9, and 12 months. The individual atlases from the infant participants were then used to create average age-specific macroanatomical atlases of 83 (Hammers) segments and 56 (LPBA40) segments, respectively.

The third objective was to examine the validity of the atlases. We tested the internal validity of the automatically-generated macroanatomical atlases against each individual's manually segmented atlas, both for atlases created directly on the participant's brain, and for the age-appropriate average atlas transformed into the participant space. To examine how atlas fit changed across age ranges, we also tested individual participants' manually segmented brain regions against an "age-appropriate" average MRI template and against templates based on ages older than the participants (from next oldest infant atlas through adult-based atlases). Finally, we examined external validity by testing the age-based template atlases against a new set of MRIs that were not used to create the atlases.

The template-based atlases constructed in the current study are available online (http://jerlab.psych.sc.edu/NeurodevelopmentalMRIDatabase/, [10]).

2. Materials and Methods

2.1 Participants, MRI Acquisition, and Average MRI Templates

The participants, MRI acquisition, and average MRI templates came from existing datasets, both from our lab and others ([5];[10]; see Supplemental Information). The MRI images for the anatomical atlases came from the University of South Carolina McCausland Center for Brain Imaging (USC-MCBI). The averages were done at ages 3, 4.5 6, 7.5, 9 and 12 months, and were based on 10 to 14 subjects at each age. The procedures for MRI acquisition are described elsewhere (USC-MCBI,[5];[10]). The relevant MRI type for the current paper was a T1-weighted scan collected on a Siemens Medical System 3T Trio with a 3D T1-weighted MPRAGE RF-spoiled rapid flash scan in the sagittal plane (1 mm^3 resolution, covering the entire head). The average templates were constructed on the MCBI 3T T1-weighted images with an iterative procedure [9, 15-17] and non-linear registration methods (using Advanced

Normalization Tools, ANTS;[18]; [19]). The resulting average MRI template is an unbiased representation of the infant brain average. The average MRI templates are available online (http://jerlab.psych.sc.edu/NeurodevelopmentalMRIDatabase/).

We also used MRI images for the external atlas validation from the NIH MRI Study of Normal Brain Development (NIHPD). The NIHPD MRI images were from the Objective-2 sample, and were selected for infants who were within ± 2-weeks of ages 3 (N = 21, 10F/11M), 6 (N = 32, 15F/17M), 9 (N = 29, 16F/13M), or 12 (N = 25, 11F/14M) months of age. Detailed methodology for the NIHPD Objective-2 can be found in publications [20, 21], as well as from the Objective-2 Procedure Manuals available at the NIHPD Database Repository website (https://nihpd.crbs.ucsd.edu/nihpd/info/index.html). The NIHPD scans were collected with Siemens Medical Systems (Sonata, Magenatom) and GE Systems (Signa Excite) 1.5T scanners at two different sites and were a 2D scan in the axial plane (1 × 1 × 3 mm resolution)

2.2 Anatomically-Labeled Stereotaxic Atlas Creation

Four sets of atlases were created (Table 2). These included: 1) Manually delineated atlases for each of the average 3T MRI templates at ages 3, 4.5, 6, 7.5, 9, and 12 months, 2) Manually delineated atlases for 20 individual participants (used for internal and external validity tests), 3) Automated macroanatomical atlases for all MCBI and NIHPD participants, and 4) Automated macroanatomical atlases for the 3T MCBI average templates.

Manually Delineated Atlases: Average-Templates—The manually drawn template atlases were constructed by manual delineation of fourteen areas on each average MRI template. Adaptations of the LONI manual segmenting protocol was used to define the lobar areas (frontal, temporal, parietal, occipital and insular), sub-lobar areas (fusiform, cingulate) and subcortical areas (cerebellum, brainstem, thalamus, corpus callosum, and striatum;[2]), as well as the ventricles. Our manual delineation sequence is listed in Table 3. The resulting areas were put in a single MRI volume, with the sub-lobar areas masking out the corresponding voxels from the lobar areas; we also retained each area in a separate MRI volume. An atlas was constructed for each of the 3T average MRI templates for the infant ages (3, 4.5, 6, 7.5, 9, and 12 months). The atlases were delineated by one individual and compared against the delineation of a second observer for six areas (brainstem, cerebellum, thalamus, frontal, temporal, occipital). Over the six infant ages and six brain areas the overlap of the final average template atlas and the test observer was 0.973, and the median Dice agreement between the two observers was 0.958 (range = 0.89 to 0.99).

Manually Delineated Atlases: Individual Participants—Selected participants had manual delineation done for three non-cortical areas (cerebellum, brainstem, and thalamus) and three cortical lobes (frontal, temporal, and occipital). The delineation for the individuals was done in the same manner as the average templates. Two of the participants at each infant age from the MCBI MRIs were randomly chosen as test participants for manual delineation. Two participants from the NIHPD MRIs at 3, 6, 9, and 12 months were also chosen for manual delineation. Thus, there were four manually delineated participants at 3, 6, 9, and 12 months; and two manually delineated participants at 4.5 and 7.5 months of age.

The manual delineations were done by several individuals and compared against the delineation of a single observer for six areas (brainstem, cerebellum, thalamus, frontal, temporal, occipital). Over the 20 participants and six brain areas the overlap of the final average template atlas and the test observer was 0.943, and the median Dice agreement between the two observers was 0.880 (range = 0.84 to 0.93).

Automated Macroanatomical Atlases: Individual Participants—Four atlases were constructed on the individual participants MRIs, based on two independent sets of labeled brain images, and two registration types. The adult brain segmentations from www.brain-development.org (Hammers atlases; [12, 22, 23]) were used as one atlas, and the LONI Probabilistic Brain Atlas segmentations (40 individuals, 56 manually delineated areas; LPBA40;[2]) were used for the other atlas. Each individual infant MRI's extracted brain was registered (both linearly and non-linearly) to each of the adult brains (both Hammers and LPBA40) and each labeled adult atlas was transformed to the individual infant space. These labeled sets (e.g. 30 individuals, for Hammers atlas) of linear transformed atlases were then fused in a majority vote procedure ([7, 11]; see Supplemental Information). The resulting atlas identifies the majority-voted brain segment for each voxel of the individual infant brain. The same procedure was done separately for both sets of labeled atlases. Therefore, each infant participant had a linear Hammers atlas, a nonlinear Hammers atlas, a linear LPBA40 atlas, and a nonlinear LPBA40 atlas.

Automated Macroanatomical Atlases: Average Templates—The Hammers and LPBA40 labeled atlases were constructed for the average MRI template from a majority vote procedure, using the individual participants from whom the average was made. For example, for the 3-month average template, each of the 14 MCBI infants at 3 months of age were registered (both linearly and non-linearly) to the 3-month old average template and the majority vote fusion procedure was used to construct both Hammers and LPBA40 atlases. The Hammers and LPBA40 atlases for each participant were then transformed separately by both linear and nonlinear registration parameters to the average MRI template space, and the resulting individually transformed atlases were fused with the majority vote procedure ([11]; [24]) to construct the labeled average MRI template stereotaxic atlas. Thus, as with the individual participants, each average MRI template had a linear Hammers atlas, a nonlinear Hammers atlas, a linear LPBA40 atlas, and a nonlinear LPBA40 atlas. The NIHPD participants at 3, 6, 9, and 12 months were not used to create these averages and were reserved for an external validation of the atlases.

2.3 Linear and Non-linear Registration

Linear and non-linear registration methods were used in the construction of the atlases and in our evaluation tests. For linear registration, the FMRIB's Linear Image Registration Tool from FSL (FLIRT;[25]) was used to register the MRI brain volume of the participant to a reference brain volume (infant participant to segmented adult atlases for participant macroanatomical atlas; infant participant to average MRI template for average template macroanatomical atlas). The FLIRT procedure was done with a 12-dof affine search, and cost and searchcost used the “corratio” algorithm. The linear registration produces a linear affine transformation matrix that can be applied to MRI volumes in the participant's space

(e.g., individual participant atlas) to transform the volume to the reference space, and an inverse transformation matrix can be applied to MRI volumes in the reference space (e.g., adult manually segmented atlas) to transform the volume into the participant space. Advanced Normalization Tools (ANTS;[18]) was used for nonlinear registration. The ANTS version 2.1.0 was used, with the antsRegistration procedure and the cross-correlation metric, to a 1 mm voxel resolution, and the SyN transform (gradient step 0.1).

3. Results

Several individual and average atlases were successfully created. Manually delineated template-based atlases were created for each target infant age (3, 4.5, 6, 7.5, 9, and 12 months). Figure 1 shows the manual template on the six infants ages (1A-sagittal; 1B-axial), along with the manual template for the atlas of the young adults (see Supplemental Information for young adult work). Figure 2a shows 3D color rendering of the manual atlas overlaid on the average MRI template for each infant age, and the young adults. For selected participants at each age, the six manually delineated brain areas were done (cerebellum, brainstem, thalamus, frontal lobe, temporal lobe, occipital lobe). Figure 2b shows a 3D color rendering of these six areas on one 3-month-old participant. The Hammers and LPBA40 macroanatomical atlases were done for all individuals (MCBI and NIHPD). Figure 3a shows the Hammers and LPBA40 atlases on a 3-month-old individual and a 12-month-old individual. Figure 3b shows the Hammers and LPBA40 atlases on the MRI templates for the 3-month-old and 12-month-old infants. Figure 4 shows axial slices of the average MRI template for the 6-month-old participants, along with slices at the same level for the manual atlas, Hammers atlas, and the LPBA40 atlas. The template-based atlases constructed in the current study are available online (http://jerlab.psych.sc.edu/NeurodevelopmentalMRIDatabase/,[10]). This includes the manual lobar atlas, the LPBA40 atlas, and the Hammers atlas for each age-appropriate average MRI template.

The overlap of the manually drawn atlas and the Hammers and LPBA40 atlases were examined for infant atlases to evaluate the overlap of the manual and the two automatically generated atlases. The overlap between the areas of the manual atlas and the Hammers and LPBA40 atlases are given in Table 4. We used the overlapping areas found in Table 4 to recode the individual participant Hammers or LPBA40 atlases into comparable manual atlas areas for some of the analyses. For these analyses, we did not examine the manually defined occipital lobe because of the disparity between our definition and corresponding LPBA40 / Hammers atlases. Additionally the LPBA40 atlas did not delineate the thalamus.

3.1 Manually delineated regions versus registration/transformation to template atlases of various ages (Table 5, Comparison 1)

Table 5 is a summary of our comparisons. The first analysis examined the effect of age-appropriate atlases, by looking at the overlap between the manually delineated region of an individual, with the regions resulting from registration / transformation to the age-appropriate atlas and to all older age template-based atlases (all infant ages, 2 years, 12 years, 18 years, 20-24 years). This was done for the participants with manually delineated regions. The line graphs in Figure 5 show the mean Dice value as a function of the age of

the template-based atlas separately for each age group. The registration / transformation for panel A was the linear registration, with the non-linear registration shown in panel B. Each sub-panel shows the results for one of six different brain regions. In almost all cases the age-appropriate registration / transformation areas provided the largest overlap with the manually delineated regions of an individual. There was a gradual decrease on the Dice overlap as the difference between the participant age and the template age increased. The analogous results for the nonlinear registrations were similar for all areas except the brainstem and thalamus. The nonlinear registrations seemed to eliminate the age effects for these segments.

We compared the fit of the age-appropriate infant atlas, the atlas from the 2-year-old children, and the adult atlas. The bar graph in Figure 6 shows the mean Dice value as a function of the brain region with a bar for each age of the template-based atlas (same age as participant, 2 years, or 20-24 years), for both linear and nonlinear registrations. The Dice value was analyzed with an Age (3: age-appropriate, 2-year-old, 20-24-year-old) X Registration Type (Linear, Nonlinear) X Segment (6: cerebellum, brainstem, thalamus, frontal lobe, temporal lobe, and occipital lobe) ANOVA. There was a significant main effect of age, F (2, 38) = 131.24, $p < .0001$, such that overlap was higher between the manually delineated regions and registration/transformation to the age-appropriate atlas (M = 0.851, SE = 0.0022) than registration/transformation to either the 2-year-old (M = 0.812, SE = 0.0028) or 20-24-year-old (M = 0.809, SE = .0026) atlases. There was also a significant main effect of segment, F (5, 95) = 40.81, $p < .0001$. There was no main effect of registration type, but there was a significant 3-way interaction between age, registration type and segment F (10, 190) = 27.61, $p < .0001$. We used the Scheffe' post hoc correction procedure to examine this interaction separately for linear and nonlinear registrations. For linear registration, the age effect was significant (e.g., age-appropriate templates performed better than those for older ages) for all six brain areas (Figure 6, left panel). For nonlinear registration, the cerebellum, frontal, occipital, and temporal lobes showed significant age effects, whereas the age effect for the brainstem and thalamus comparisons was not significant (Figure 6, right panel). The nonlinear transform resulted in larger Dice values for the thalamus and brainstem segments.

3.2 Manually delineated regions versus individual and average macroanatomical atlases (Table 5, Comparison 2)

The second analysis was to examine the overlap between the manually delineated region for each individual, with the regions from that individual's Hammers and LPBA40 atlases, and with the regions from an age-appropriate MRI template atlas transformed into that participant's MRI space. This was done for the participants with manually delineated regions. The Hammers and LPBA40 atlas segments were recoded into regions equivalent to the manual atlas areas in order to compare the regions defined by the manual atlas with comparable regions defined by the average template macroanatomical atlases. This was accomplished by using any atlas segment where the overlap between the manual atlas and the target atlas area was greater than 0.5 (Table 4). The first ANOVA used data provided by the Hammers atlases. The Dice value was analyzed with an Age (6: 3, 4.5, 6, 7.5, 9, 12 months) X Segment (5: cerebellum, brainstem, thalamus, frontal lobe, and temporal lobe) X

Registration Type (2: linear, non-linear) X Atlas Source (2: participant, average-transformed) ANOVA. There were significant effects of the registration type, $F(1, 14) = 144.8$, $p < .0001$, and atlas source, $F(1, 14) = 15.82$ $p = .0014$. The Dice coefficients from the non-linear analysis were larger than the nonlinear ($N = 200$, M's 0.843 and 0.782, SE = and 0.0043 and .0058, respectively) and the Dice coefficients from the individual participant atlas were larger than those from the age-transformed atlas ($N = 200$, M's = 0.809 and 0.779, SE = and 0.0048 and .0053, respectively). It is interesting that the interaction between these two factors was not statistically significant, indicating that the linear/nonlinear change in the Dice coefficient was the same for the age-appropriate average-transformed comparison and the individual macroanatomical atlas comparison. For the ANOVA on the LPBA40 data, there were also significant effects of the registration type, $F(1, 15) = 78.84$, $p < .0001$, and atlas source, $F(1, 15) = 26.46$, $p = .0014$; similar patterns were present in the means to those described for the Hammers data.

There was a three way interaction between the registration type, atlas source, and segment, for both Hammers and LPBA40 atlases, $F(4, 56) = 14.07$, $p < .0001$ and $F(3, 42) = 6.77$, $p < .0001$, respectively. Figure 7 shows the mean Dice value for the Hammers and LPBA40 atlases for the five segments, the linear and non-linear registrations, separately for the participant atlas and the average-transformed atlas. The interaction was due to the size of significant effects, rather than the specific pattern. For both the transformed age-appropriate-average atlas and the participant atlas, the nonlinear Dice coefficient was larger than the linear Dice coefficient for both the brainstem and thalamus segments. This difference between nonlinear and linear coefficients also occurred for the participant atlas source for the cerebellum segment. Otherwise, all the other segments did not have significantly Dice coefficients for linear and nonlinear registration methods.

3.3 Individual macroanatomical atlases and registration/transformation to average macroanatomical atlas (Comparison 3)

The final analysis examined the overlap between the Hammers or LPBA40 atlases that were constructed on the individual, with the segments coming from a registration / transformation from the average atlas to the participant MRI volume space. These atlases were constructed for all infant MRIs. The analysis came from the participants who contributed to creation of the average atlas to verify the internal validity of this approach. The analysis also used the MRIs from the NIHPD infants, who were not included in creation of the averages, as an external validation of the usefulness of the average atlas. A Dice coefficient was calculated between the average-transformed and the participant atlas by defining the intersection as the agreement for each voxel over all segments of the macroanatomical atlas, thus providing a measure of overall fit between the two atlases.

The multiple-segment Dice coefficient was analyzed with an Age (6) × Group (2: MCBI, NIH) × Registration Type (2) ANOVA, separately for the Hammers and LPBA40 atlases. Figure 8 shows this overall comparison for the Hammers and LPBA40 atlases, separately for the linear and nonlinear methods and the two groups. It can be seen in this figure that the fit between the transformed and participant atlases were similar for the two groups, and were generally about 0.90. There was a significant main effect for the registration type, $F(1, 165)$

= 165.14, p < .0001, and the testing group factor was close to significant, F (1, 165) = 3.16, p = .0736. The Dice coefficient for the MCBI infants was larger than the NIH infants (M's = 0.937 and 0.899, SE's = .0017 and .0012, respectively), and the linear methods resulted in a larger Dice coefficient than the nonlinear method (M's = 0.929 and 0.898, SE's = 0.0084 and 0.0077, respectively). There were no other main effects or interactions.

We also calculated the 'target overlap' ([26]) for the two atlases. The target overlap represents the intersection a target and reference overlap, divided by the reference volume area. This represents the sensitivity of the analysis, and is a measure of segment concordance when there are some areas in the reference segment not fully represented in the target segment. Figure 8 shows the target overlap for the age-transformed and the participant volumes, calculated over all the segments. The target overlap for both MCBI and NIH participants was about 0.95, indicating a very close fit between the average age-transformed and individual participant atlases. An Age (2) × Group (2) × Registration Type (2) ANOVA showed only a significant effect for the registration type factor; the target overlap for the two groups was not significantly different. Finally, we also calculated the target overlap for the 83 areas of the Hammers atlas and the 56 areas of the LPBA40 atlas. Figure 9 shows the target overlap separately for the MCBI and NIHPD groups for the linear registration/ transformation, and for all the segmented areas of these atlases. There was a good correspondence between the MCBI and the NIHPD groups on the pattern of target overlap across the different segments for both the Hammers and the LPBA40 atlases.

4. Discussion

Previous neuroanatomical stereotaxic atlas work in infants has focused either on newborns [27-29] or a few limited ages [7, 11]. The current work provides viable alternatives for stereotaxic atlas work with infants from 3-12 months of age with fine-grained ages. We created age-specific stereotaxic atlases for average MRI templates for infants. This was done by manual delineation of average MRI templates (from[5]). Transforming the average atlas to individual participant MRI space and comparing the overlap of the transformed atlas to manual delineated regions on individual participants tested the validity of the template-based atlases. The overall overlap between the transformed atlas regions and the manually delineated regions was very good (Dice values ~ 0.85). The largest overlap was with the delineated regions and an atlas from an age-appropriate average MRI template. There was decreasing overlap between the manually delineated regions and the template-based atlas regions as the age difference between the participant and the average atlas increased. Using an age-appropriate template-based atlas provided significantly higher overlap than using an adult template-based atlas. Overall, these results suggest that automatic atlas segmentation is best done using age-appropriate stereotaxic atlases. The overlap values found with the manually delineated atlases and the internal / external validation comparisons are comparable to work done with adult anatomical atlases based on similar procedures (e.g. [2]; [11]). We thus expect that our atlases should perform as well as these adult atlases.

A second objective of the current work was to use the procedures found in Gousias et al. ([11]) to create individual macroanatomical atlases for infants from 3-12 months. This approach worked similarly for infants across the first year, and worked similarly for the

Hammers atlas and the LPBA40 atlas. This procedure should be useful for automatic computation of individual macroanatomical atlases for infant participants. It is possible that a direct registration / transformation from the average to an individual may be sufficient. The overlap between the individual macroanatomical atlases and registration/transformation to an age-appropriate average macroanatomical atlas did not change substantially over age. The values of the Dice coefficients were around 0.90, and the overlap values were near 0.95. These results were similar when tested with an external validation group. The computational requirements of the Gousias et al. ([11]) procedure are quite high, so the use of the average anatomical atlas for automatic computation may suffice for some applications.

There were differences in fit across anatomical regions. For example, the cerebellum and frontal lobes showed better overall fits for the manual atlas, compared with the thalamus, occipital lobe, and temporal lobe (Figures 6, 7). The areas with lower overlap also were more strongly affected by the use of the atlas from the age-inappropriate MRI template (e.g., occipital lobe, thalamus, Figures 5, 6). Additionally, the occipital lobe region had small Dice values for all participants with the child and adult average templates, whereas the other regions showed larger Dice values for the older infants and these older templates (i.e., last four points in Figure 5). The nonlinear registration improved the fit between the participant manually delineated segments and the age-appropriate MRI template segments, as well as segments from older ages (e.g., Figure 6). These results may be helpful in determining whether to use automatic atlas procedures or manual delineation. For some regions (e.g., frontal lobe, cerebellum) the automatic segmentation may provide results comparable to manual delineation. For others, only manual delineation of segmented areas will provide adequate identification of brain areas. The nonlinear registration improved the fit between the individual participants and either the age-appropriate manual segments or the age-appropriate macroanatomical atlases, particularly for those areas that had lower Dice values from the linear registration.

Some of our comparisons may be described as internal validations of the procedures, whereas others are external tests of the atlases. For example, our comparison of the manually delineated regions against the registration / transformation to the template atlas (Table 4, Comparison 1) used four participants at 3, 6, 9, 12, and 24 months. Two of these participants also were used to construct the average MRI template upon which the manual delineations were made (MCBI participants), and two were not used in the construction of the template (NIHPD participants). We found similar results for the internal validation of the MCBI participants against their age-appropriate atlas and the external validation of the NIHPD participants against their age-appropriate atlas. Both the internal and external validation participants showed a closer fit to the age-appropriate atlas than to the atlases based on older groups (e.g., 2-year-old or adult atlas; see Figure 5, Figure 6). Similarly, the comparison of the majority vote fusion age-appropriate average atlas with the registration / transformed atlas was done both with the MCBI participants (Table 4, Comparison 3, Internal) and NIHPD participants (Table 4, Comparison 3, External). The results from the internal validation comparisons were nearly identical in the pattern of the results with the external validation comparisons, with slightly higher Dice coefficients for the internal validation (Figure 8). Also, the pattern of overlap across the individual segments of the Hammers and LPBA40 atlases was very similar for the MCBI and the NIHPD groups

(Figure 9). An important note for the external validation sample is that it was composed entirely of 1.5T, 2D, 1 × 1 × 3 mm scans. These scans have poorer spatial resolution due to the smaller magnet strength, the 2-D sampling, and the thicker slices. The similar performance of the validations with the external and internal validation comparisons implies these atlases will generalize to a wide range of scanning protocols. The slightly smaller Dice coefficients for the external validation comparisons likely represent the level to which these results will generalized to a new sample of MRIs; though we expect that MRIs with the same high-resolution characteristics as the MCBI sample may work better than the lower-resolution NIHPD MRI volumes.

These results highlight some of the limitations and advantages to different atlas approaches as they apply to infants. Gilmore et al. ([27]) and Gousias et al. ([28]) developed procedures for delineating structures on each individual newborn brain (Approach 4 in Table 1). Depending on the region of interest, automatically registering an infant to an age-appropriate atlas (Approach 2) may work well enough to eliminate the need for time-consuming individual delineation. The current work shows that automatic linear registration of a 1-year-old's brain to a 2-year-old atlas (Approach 2; e.g.[24]; or 6-month-old to MNI, [6]) does not work as well as registration to an age-appropriate atlas, and, there were several places where nonlinear registration improved the results. If one desires a macroanatomical atlas, one could use a majority vote approach (Approach 3; e.g. [11]) to create individual macroanatomical atlases for infant participants without needing manual delineation. Additionally, this could be done for child or adolescent groups (e.g. [30]), or even extended to studies of development in sub-cortical brain areas (e.g. [31]). However, this procedure is resource intensive. Alternatively, one could register/transform the infant participants to an age-appropriate average macroanatomical atlas, with similar precision across ages.

Our choice of 1.5-month atlas intervals across the range from 3 to 9 months resulted in about 8-14 infants for the average template at each age ([10]). We do not know if these numbers of participants in the average template resulted in less reliable templates or anatomical atlases for each age. However, we prefer the approach of having smaller age ranges for our averages given the tremendous development in brain structure across the first year of life. We feel that the smaller the age range for the templates and atlases, the more likely that age-appropriate atlases will enhance both research and clinical use of these atlases. The overlap values found with both the internal and external validation procedures are comparable to work done with adult anatomical atlases based on similar procedures, so we expect that our atlases should perform as well as adult work. However, it could be preferable to obtain a much larger set of infant MRIs, perhaps at one age, to examine the effect of sample size on the reliability of the anatomical atlases. These cautions apply equally to the age-appropriate average templates that exist for infant ages (e.g., [6], with 6-month-olds;[11], with 2-year olds;[5], with these ages; [24]with newborn, 12-months, 24-months).

Acknowledgements

1. Data used in the preparation of this article were obtained from the NIH Pediatric MRI Data Repository created by the NIH MRI Study of Normal Brain Development. This is a multisite, longitudinal study of typically developing children from ages newborn through young adulthood conducted by the Brain Development Cooperative Group and supported by the National Institute of Child Health and Human Development, the National Institute on Drug Abuse,

the National Institute of Mental Health, and the National Institute of Neurological Disorders and Stroke (Contract #s N01-HD02-3343, N01-MH9-0002, and N01-NS-9-2314, -2315, -2316, -2317, -2319 and -2320). A listing of the participating sites and a complete listing of the study investigators can be found at http://www.bic.mni.mcgill.ca/nihpd/info/participating_centers.html

2. The adult brain atlases from www.brain-development.org were used in the preparation of this article. (c) Copyright Imperial College of Science, Technology and Medicine 2007. All rights reserved.

3. The authors would like to acknowledge Kristen Sloan and Meagan Bang for their help with manual delineations.

This work was supported by the NIH grant, #R37 HD18942 to JER.

References

1. Richards JE, Xie W. Bensen J. Brains for all the ages: Structural neurodevelopment in infants and children from a life-span perspective. Advances in Child Development and Behavior. 2015
2. Shattuck DW, et al. Construction of a 3D probabilistic atlas of human cortical structures. Neuroimage. 2008; 39(3):1064–80. [PubMed: 18037310]
3. Altaye M, et al. Infant brain probability templates for MRI segmentation and normalization. Neuroimage. 2008; 43(4):721–30. [PubMed: 18761410]
4. Kazemi K, et al. A neonatal atlas template for spatial normalization of whole-brain magnetic resonance images of newborns: preliminary results. Neuroimage. 2007; 37(2):463–73. [PubMed: 17560795]
5. Sanchez CE, Richards JE, Almli CR. Neurodevelopmental MRI brain templates for children from 2 weeks to 4 years of age. Dev Psychobiol. 2011; 54(1):77–91. [PubMed: 21688258]
6. Akiyama LF, et al. Age-specific average head template for typically developing 6- month-old infants. PLoS One. 2013; 8(9):e73821. [PubMed: 24069234]
7. Shi F, et al. Infant Brain Atlases from Neonates to 1- and 2-Year-Olds. PLoS ONE. 2011; 6(4):e18746. [PubMed: 21533194]
8. Tzourio-Mazoyer N, et al. Automated anatomical labeling of activations in SPM using a macroscopic anatomical parcellation of the MNI MRI single-subject brain. Neuroimage. 2002; 15(1):273–89. [PubMed: 11771995]
9. Sanchez CE, Richards JE, Almli CR. Age-specific MRI templates for pediatric neuroimaging. Dev Neuropsychol. 2012; 37(5):379–99. [PubMed: 22799759]
10. Richards JE, Sanchez C, Phillips-Meek M, Xie W. A database of age- appropriate average MRI templates. Neuroimage. 2015 doi:10.1016/j.neuroimage.2015.04.055.
11. Gousias IS, et al. Automatic segmentation of brain MRIs of 2-year-olds into 83 regions of interest. Neuroimage. 2008; 40(2):672–84. [PubMed: 18234511]
12. Hammers A, et al. Three-dimensional maximum probability atlas of the human brain, with particular reference to the temporal lobe. Hum Brain Mapp. 2003; 19(4):224–47. [PubMed: 12874777]
13. Heckemann RA, et al. Automatic anatomical brain MRI segmentation combining label propagation and decision fusion. Neuroimage. 2006; 33(1):115–26. [PubMed: 16860573]
14. Song J MK, Turovets S, LI K, Davey C, Govyadinov P, Luu P, Smith K, Prior F, Larson-Prior L, Tucker D. Anatomically Accurate Head Models and Their Derivatives for Dense Array EEG Source Localization. Funct Neurol Rehabil Ergon. 2013; 3(2-3):275–293.
15. Yoon U, et al. The effect of template choice on morphometric analysis of pediatric brain data. NeuroImage. 2009; 45(3):769–777. [PubMed: 19167509]
16. Fonov V, et al. Unbiased average age-appropriate atlases for pediatric studies. NeuroImage. 2011; 54(1):313–27. [PubMed: 20656036]
17. Sanchez CE, Richards JE, Almli CR. Neurodevelopmental MRI brain templates for children from 2 weeks to 4 years of age. Dev Psychobiol. 2011
18. Avants BB, et al. Symmetric diffeomorphic image registration with cross-correlation: evaluating automated labeling of elderly and neurodegenerative brain. Med Image Anal. 2008; 12(1):26–41. [PubMed: 17659998]

19. Klein A, et al. Evaluation of 14 nonlinear deformation algorithms applied to human brain MRI registration. Neuroimage. 2009; 46(3):786–802. [PubMed: 19195496]
20. Almli CR, et al. The NIH MRI study of normal brain development (Objective-2): newborns, infants, toddlers, and preschoolers. Neuroimage. 2007; 35(1):308–25. [PubMed: 17239623]
21. Leppert IR, et al. T(2) relaxometry of normal pediatric brain development. J Magn Reson Imaging. 2009; 29(2):258–67. [PubMed: 19161173]
22. Heckemann RA, et al. Automatic anatomical brain MRI segmentation combining label propagation and decision fusion. NeuroImage. 2006; 33(1):115–126. [PubMed: 16860573]
23. Heckemann, RA., et al. Information Extraction from Medical Images (IXI): Developing an e-Science Application Based on the Globus Toolkit.. 2nd UK e-Science All-hands Conference; Nottingham, UK.. 2003;
24. Shi F, et al. Infant brain atlases from neonates to 1- and 2-year-olds. PLoS One. 2011; 6(4):e18746. [PubMed: 21533194]
25. Jenkinson M, Smith S. A global optimisation method for robust affine registration of brain images. Med Image Anal. 2001; 5(2):143–56. [PubMed: 11516708]
26. Crum WR, et al. Generalised overlap measures for assessment of pairwise and groupwise image registration and segmentation. Med Image Comput Comput Assist Interv. 2005; 8(Pt 1):99–106. [PubMed: 16685834]
27. Gilmore JH, et al. Regional gray matter growth, sexual dimorphism, and cerebral asymmetry in the neonatal brain. J Neurosci. 2007; 27(6):1255–60. [PubMed: 17287499]
28. Gousias IS, et al. Magnetic resonance imaging of the newborn brain: manual segmentation of labelled atlases in term-born and preterm infants. Neuroimage. 2012; 62(3):1499–509. [PubMed: 22713673]
29. Oishi K, et al. Multi-contrast human neonatal brain atlas: application to normal neonate development analysis. Neuroimage. 2011; 56(1):8–20. [PubMed: 21276861]
30. Hashimoto T, et al. Increased posterior hippocampal volumes in children with lower increase in body mass index: a 3-year longitudinal MRI study. Dev Neurosci. 2015; 37(2):153–160. [PubMed: 25721327]
31. Uda S, et al. Normal development of human brain white matter from infancy to early adulthood: a diffusion tensor imaging study. Dev Neurosci. 2015; 37(2):182–194. [PubMed: 25791575]

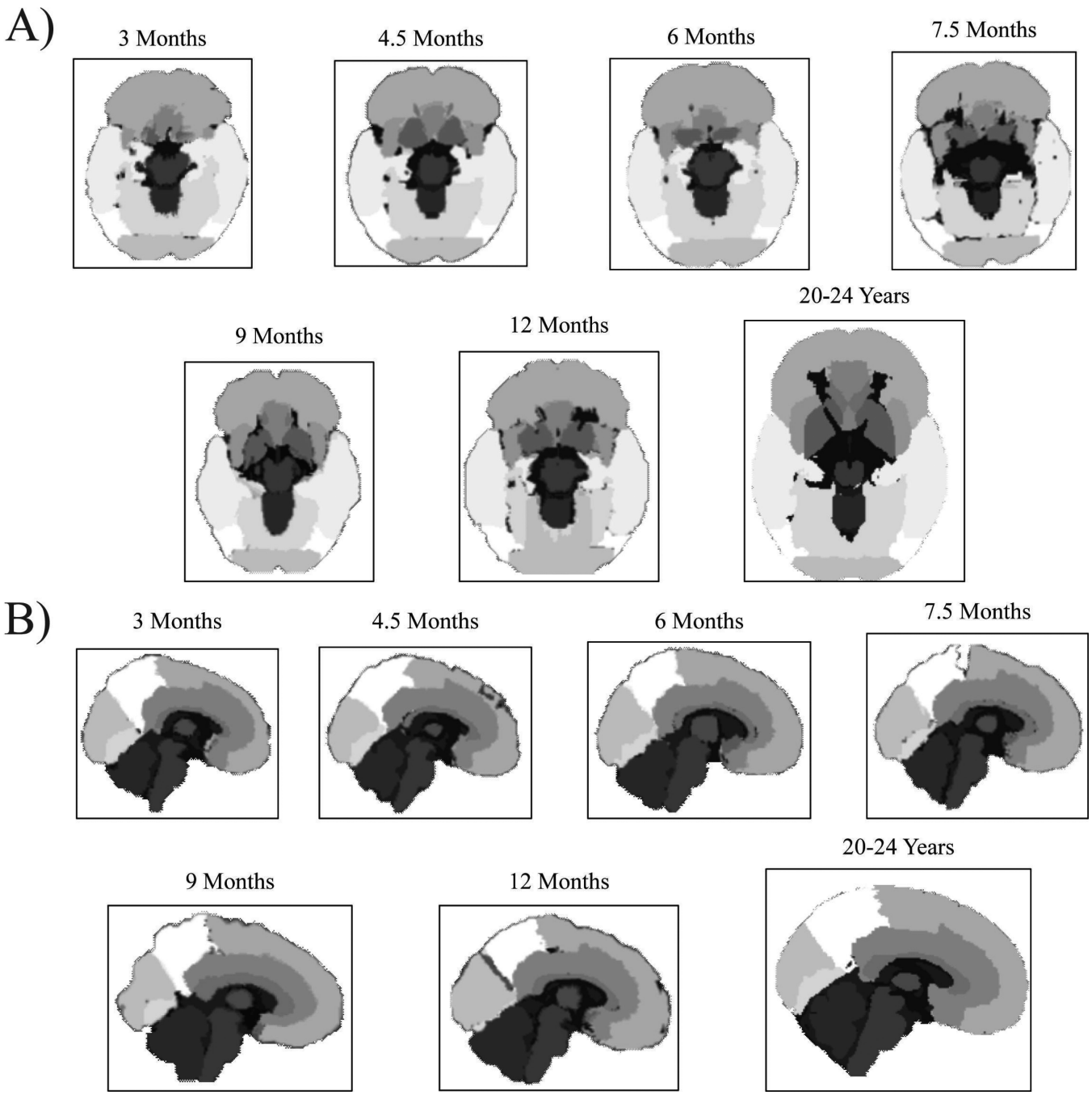

Figure 1.
Manual template-based atlas for six ages through the first year, and adult atlas. A) Axial view B) Sagittal view.

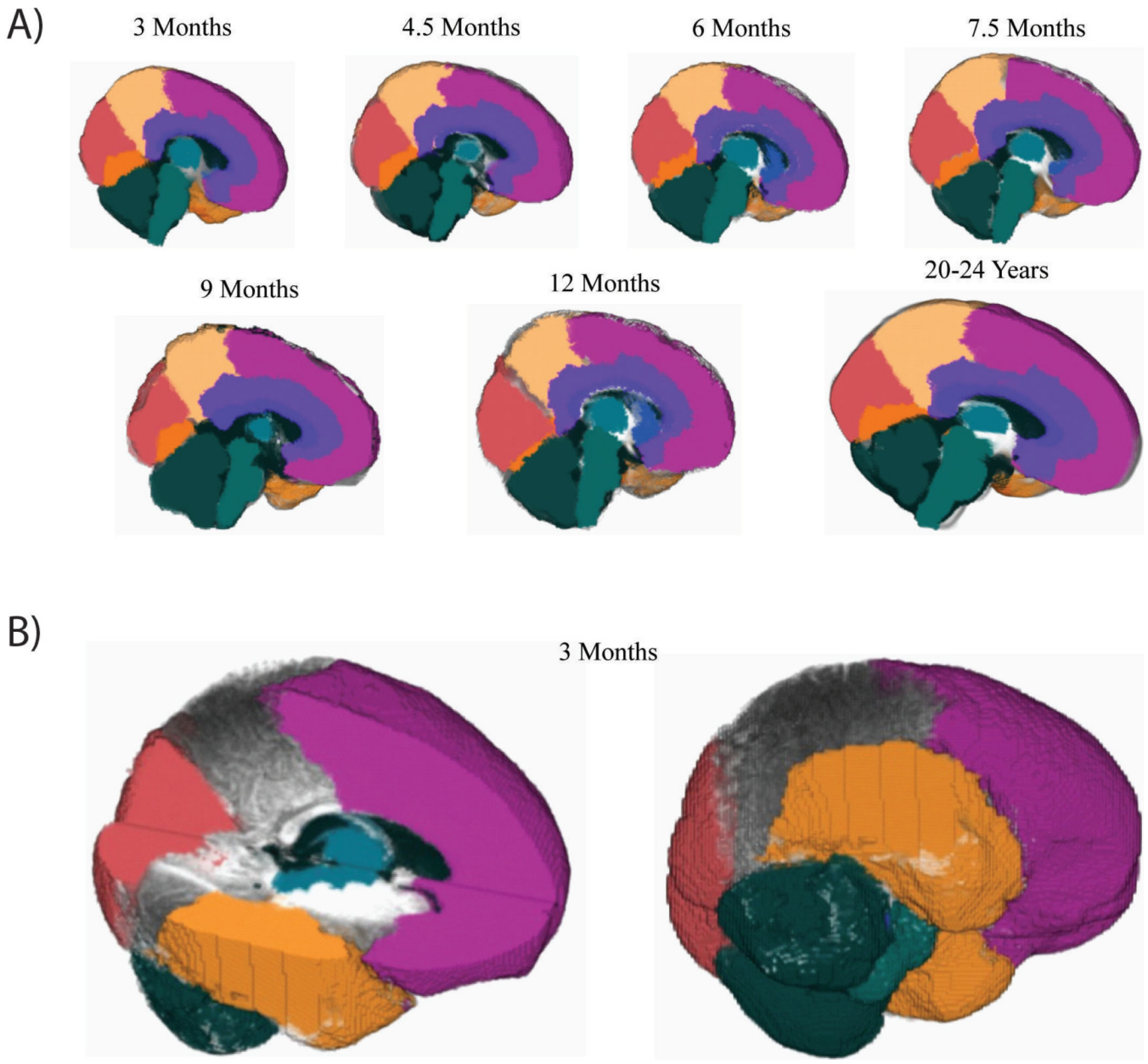

Figure 2.

A) Manual 3-D template-based atlases for six ages through the first year, and adult atlas. Presented at the mid-sagittal plane. B) Example of manual delineations on one 3-month-old infant brain. Left – medial view; Right - lateral view.

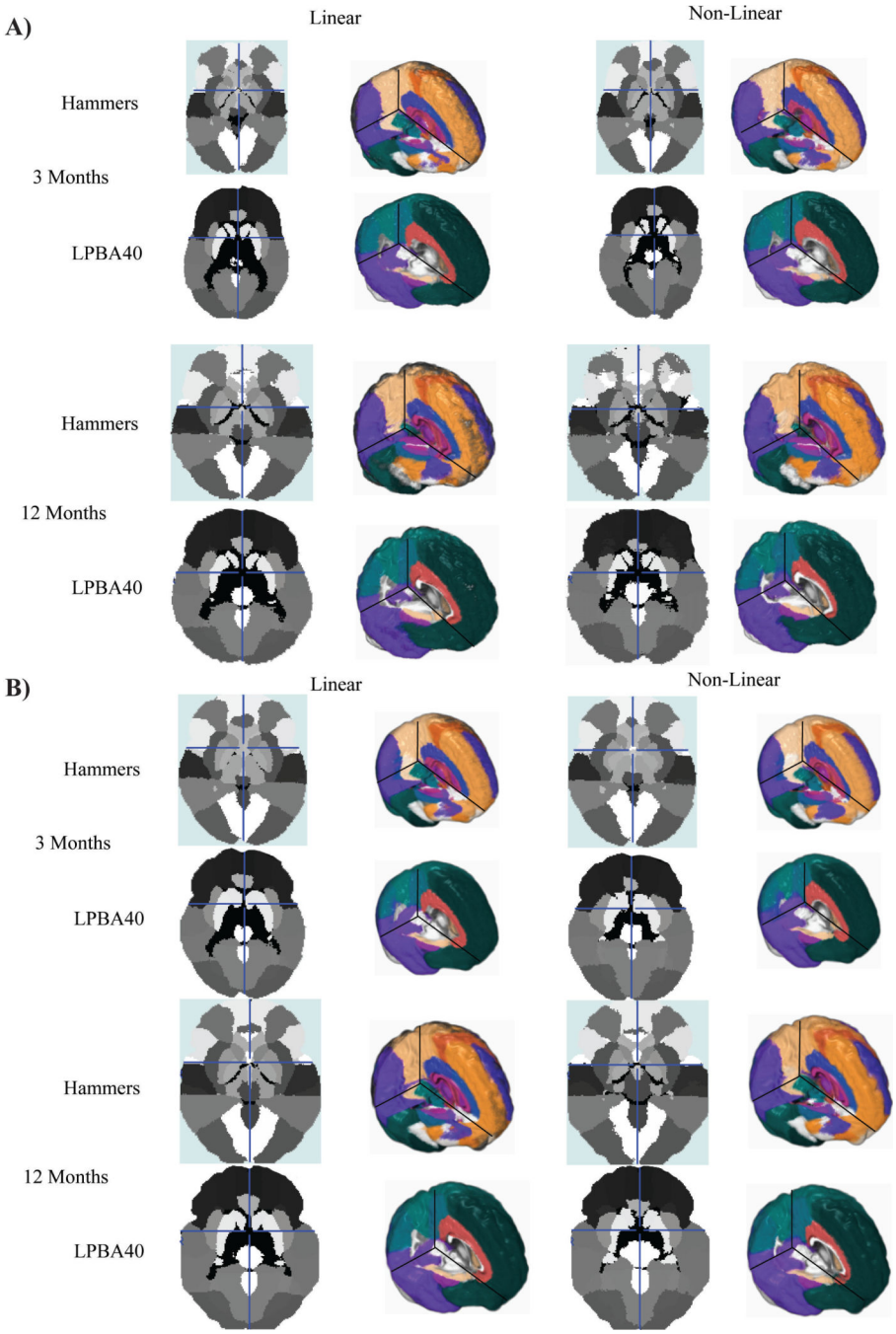

Figure 3.

Hammers and LPBA40 atlases. Axial view is shown in black and white with AC-PC line; sagittal/medial view is shown in color. A) One 3-month-old and one 12-month-old resulting from the individual majority vote procedure. B) Age-appropriate average atlases, shown on the 3 month and 12 month average templates.

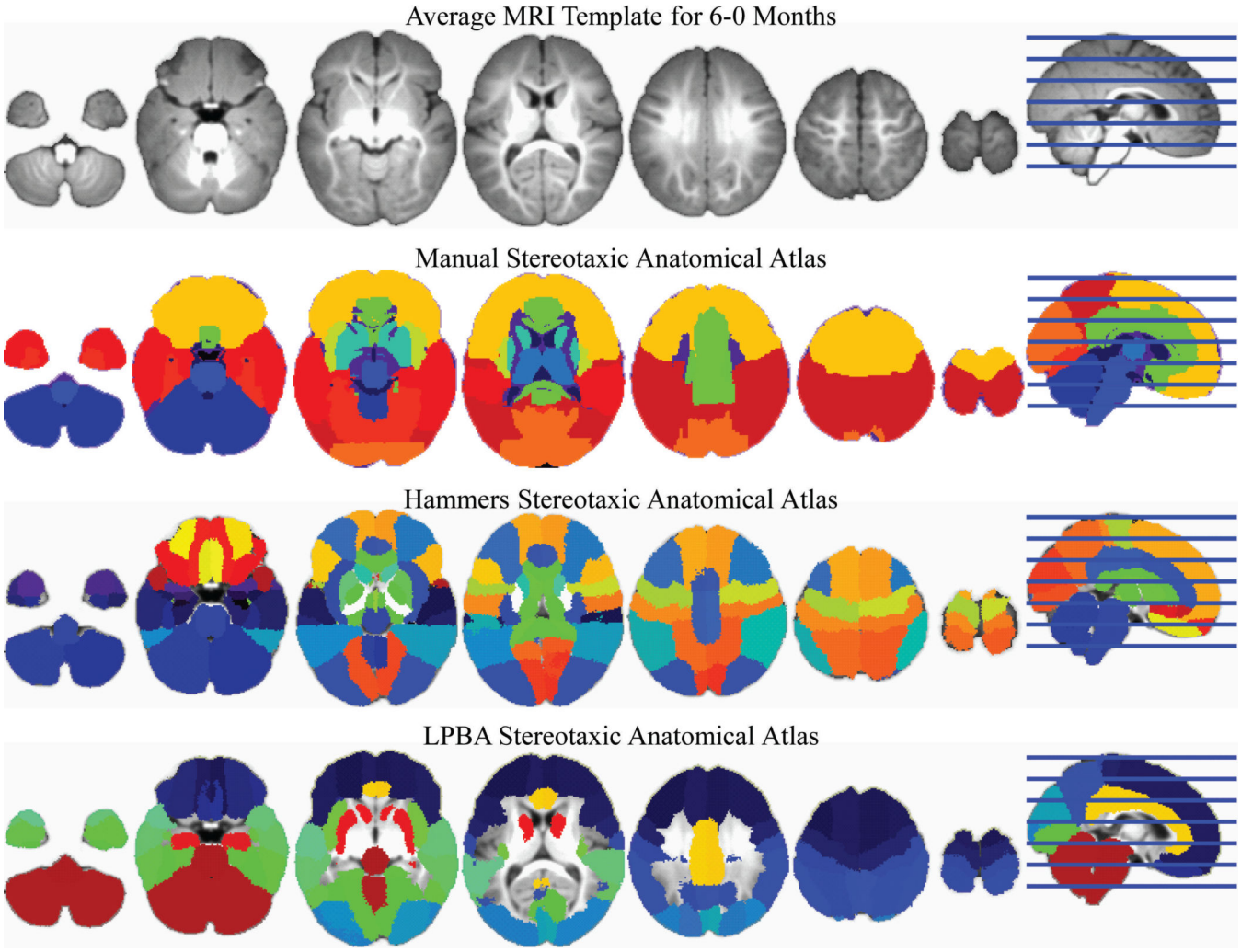

Figure 4.
Slices of average MRI template for 6-0 months participant, compared with manual, Hammers, and LPBA40 atlases.

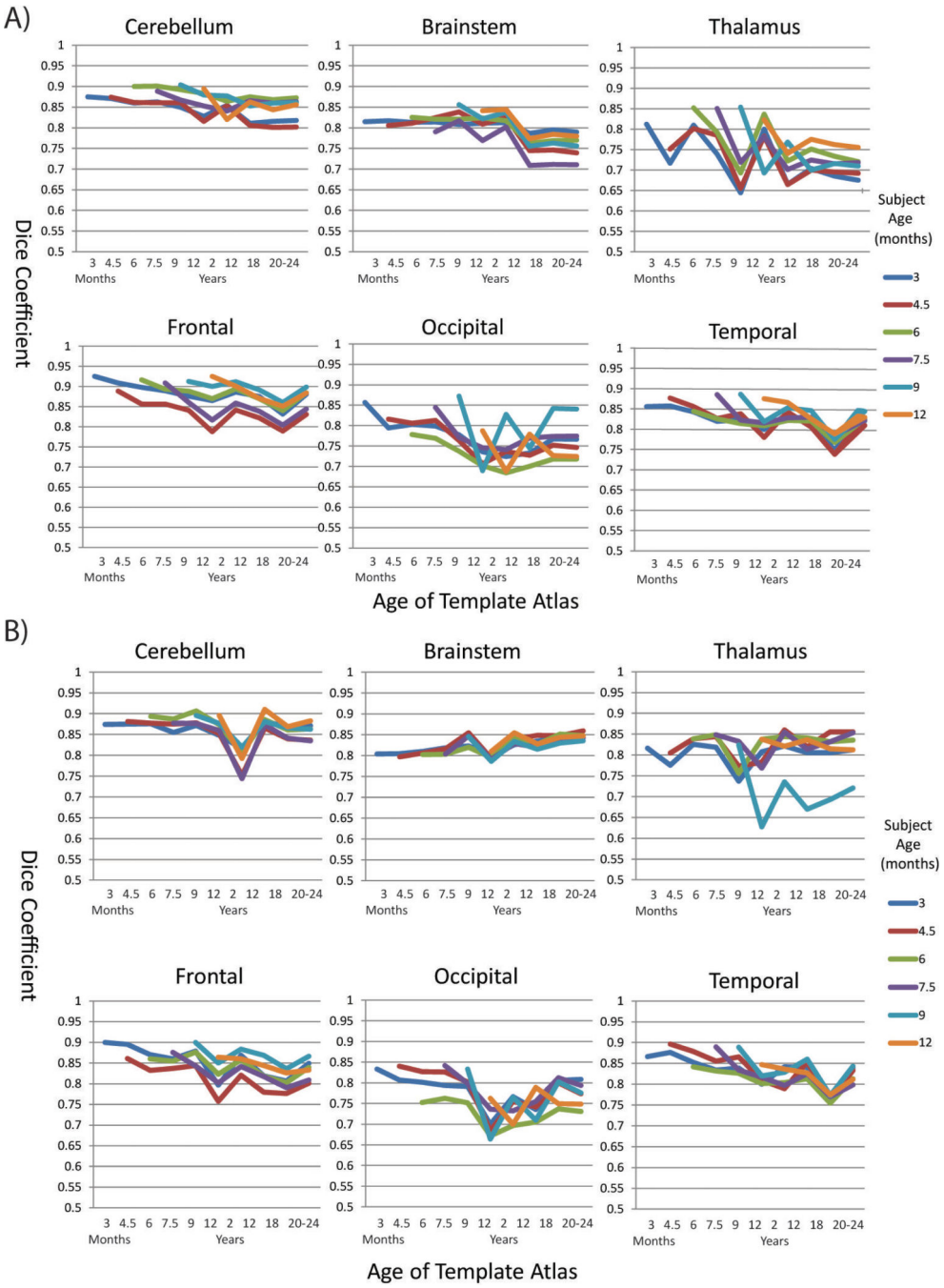

Figure 5.

Overlap between manually delineated regions and regions resulting from registration/transformation to template-based atlases. Graph shows mean Dice value as a function of the age of the template-based atlas separately for each age group. Each line represents a different age group. Panel A shows results from linear transformations, and panel B shows results from non-linear transformations, while each sub-panel shows the results for one of six different brain regions.

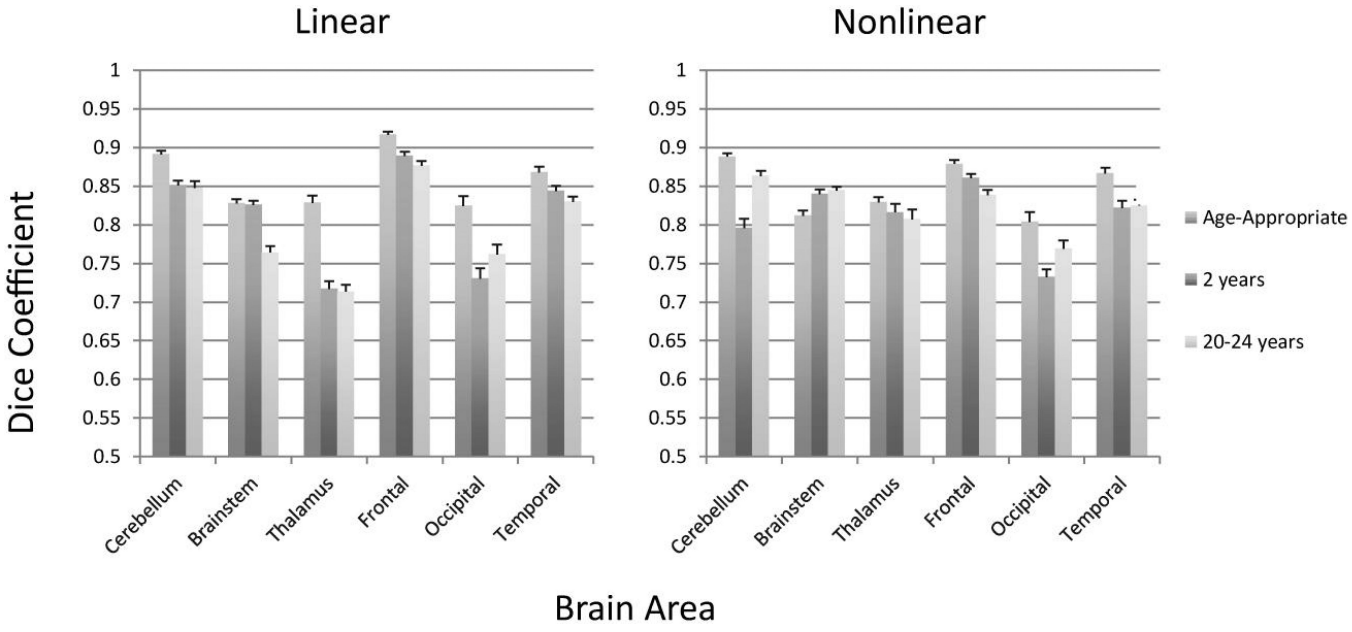

Figure 6.

Overlap between manually delineated regions and regions resulting from registration/transformation to template-based atlases. Graph shows mean Dice value as a function of the brain region with a bar for each age of the template-based atlas (same age as participant, 2 years, or 20-24 years). Error bars represent the standard error of the mean.

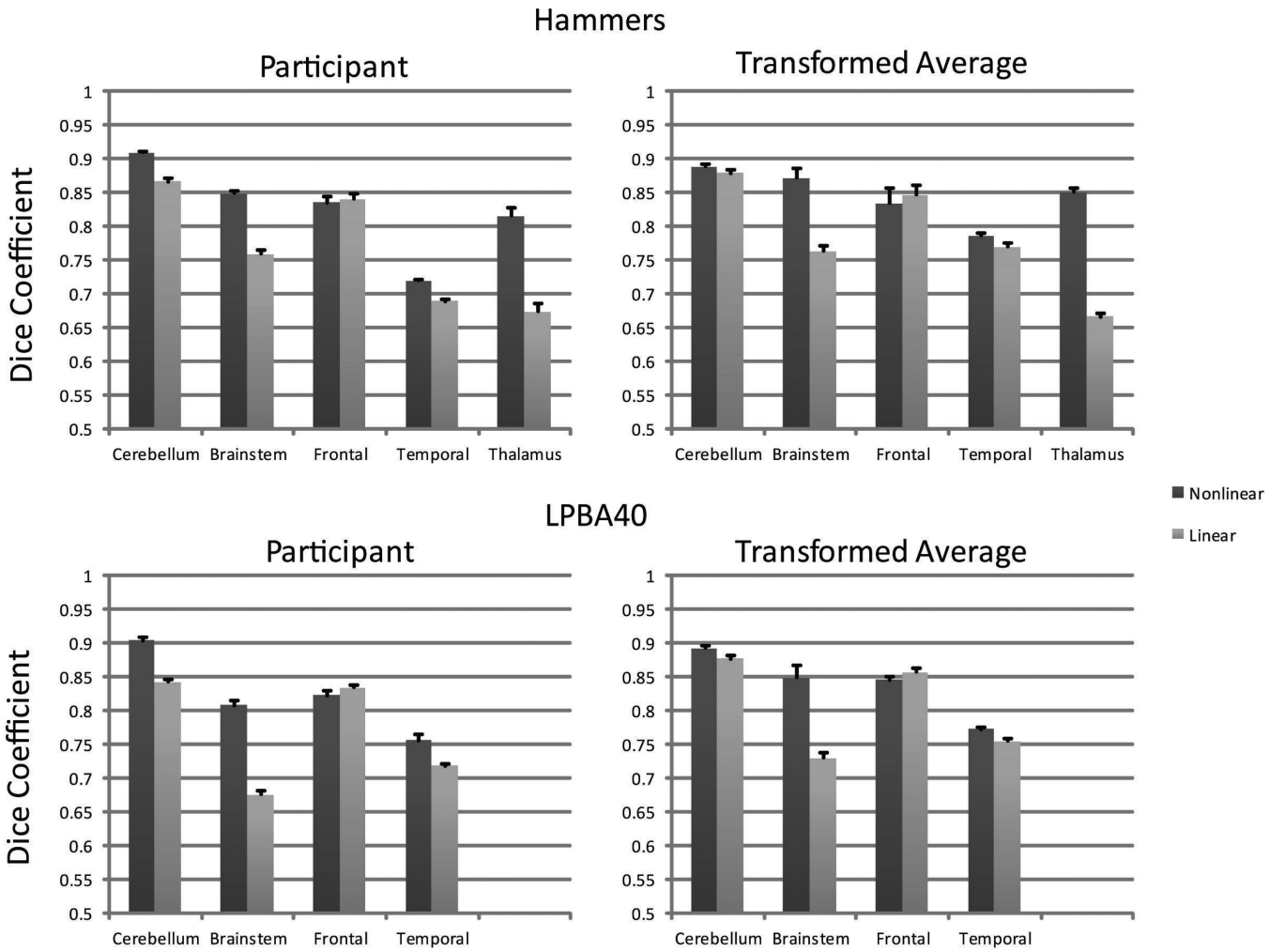

Figure 7.

Overlap between manually delineated regions and Hammers and LPBA40 atlas regions resulting from the majority vote approach to individual participant macroanatomical atlas creation (left), and the age-appropriate average MRI template atlas transformed to the participant (right). Graph shows mean Dice value as a function of the brain region and linear / non-linear registration. Error bars represent the standard error of the mean.

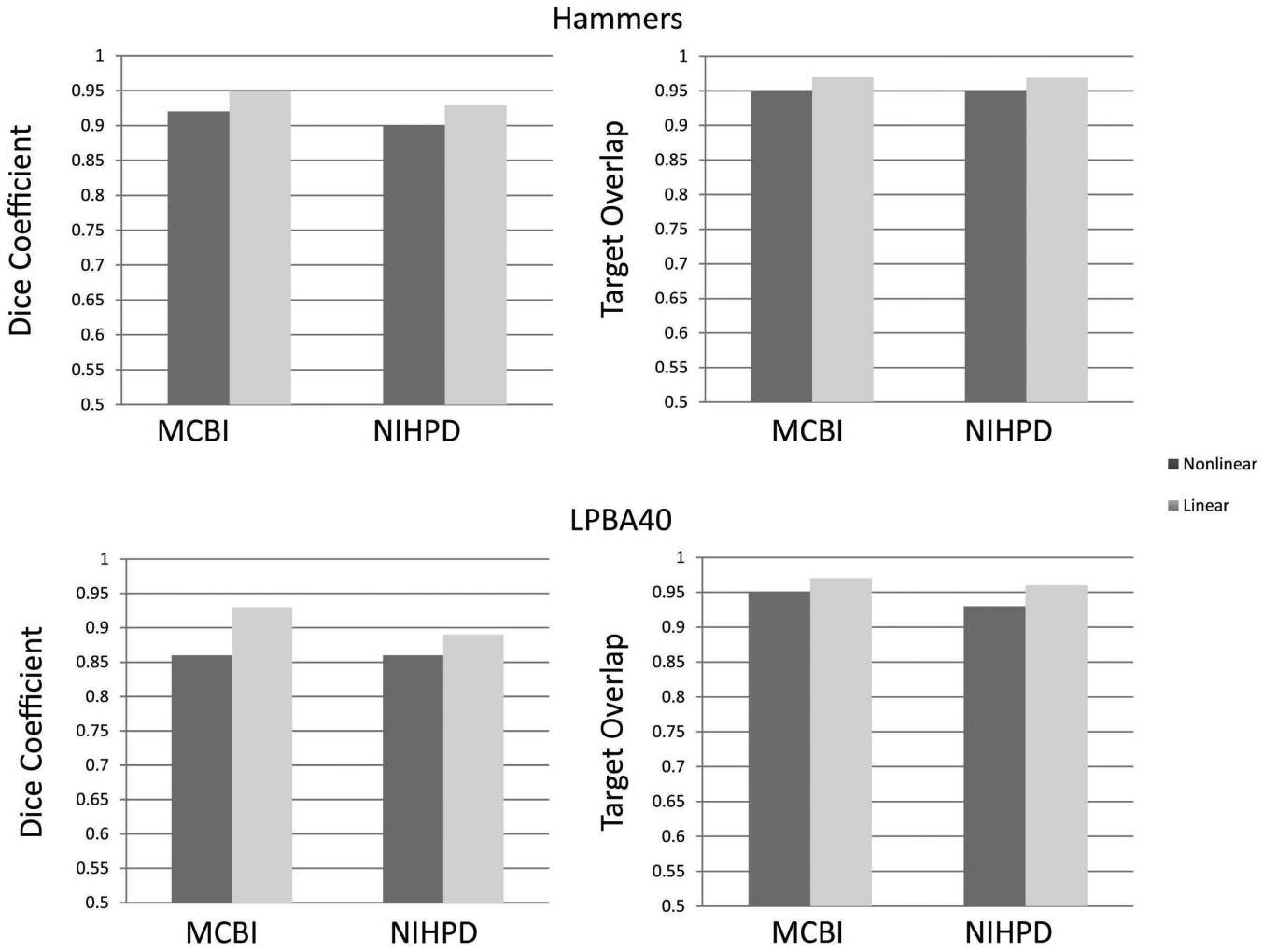

Figure 8.

Comparison of MCBI (internal validation) and NIHPD (external validation) fit between the participant atlas and age-appropriate average transformed atlas. The Dice coefficient represents the agreement between multiple segments over all the segments of the atlas, and the target overlap is the overlap of the age-appropriate average transformed atlas to the participant atlas. The SE for each graph was < .005.

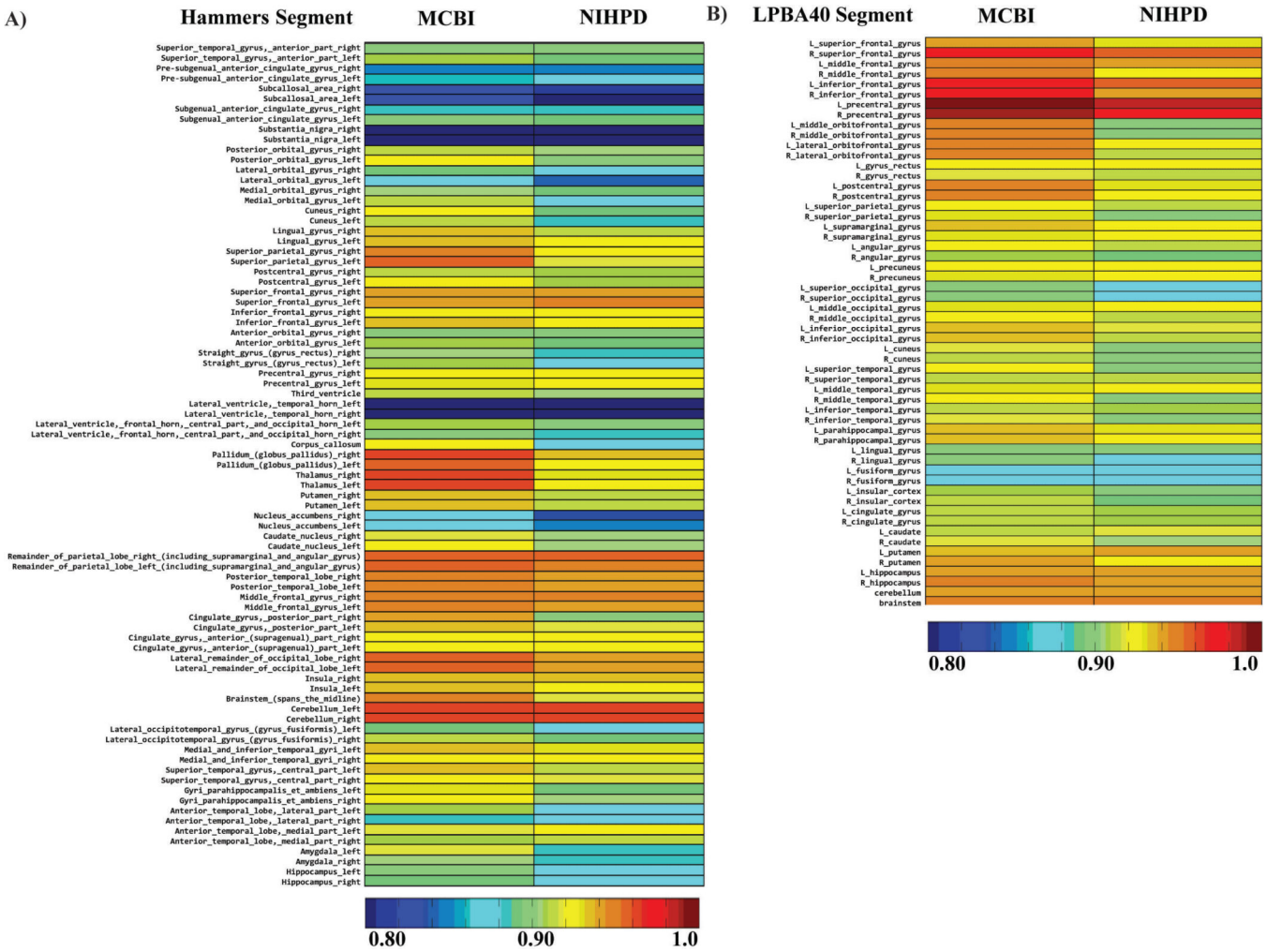

Figure 9.

Target overlap between the participant and the age-appropriate average transformed atlas, separately for the MCBI (interval validation) and NIHPD (external validation) groups. Each row represents one segment, and the color values represent the target overlap. Panel A shows data from the Hammers atlas, and panel B shows data from the LPBA40 atlas.

Table 1

Approaches to neuroanatomical segmentation using stereotaxic atlases.

Approach	Summary	Example
Hand-drawn	Anatomy hand-drawn on a single participant's or a few participants' brains and used as a guide. Visual identification on new individuals, or look-up method.	Talairach & Tournoux (1988)
Automatic-Individual	Atlases created by delineating regions on a single MRI volume. Individual images are then automatically registered to that image.	Automatic Anatomical Labeling (AAL; Tzourio-Mazoyer et al., 2002); Shi et al. (2011)
Automatic-Average	Atlases created by delineating regions on the average of many MRI volumes. Individual images are then automatically registered to that image.	Montreal Neurological Institute (MNI) structural atlas (Mazziotta, Toga et al. 2001)
Majority Vote	Manual delineation on a group of MRI volumes, followed by fusion of individual segmented with largest probability	LONI Probabilistic Brain Atlas (LPBA40; Shattuck et al., 2008); Gousias et al. (2008)

Dev Neurosci. Author manuscript; available in PMC 2015 November 14.

Table 2

The four types of atlases

Average Template Manually Delineated Atlas
Manual delineation of 14 lobar and sub-lobar areas for each average MRI template (3, 4.5, 6, 7.5 9, and 12 months). This is an average atlas that may be used for automatic atlas registration / transformation to individual participants. (Table 1, Automatic-Average)
Participant Manually Delineated Atlas
Manual delineation of 14 lobar and sub-lobar areas for 20 selected participants (2 MCBI 3.T MRIs ea at 3, 4.5, 5, 7.5, 9, and 12 months; 2 NIHPD 1.5T MRIs each at 3, 6, 9, and 12 months). This is to provide a “gold standard” against which to validate the average template manually delineated atlas, and the automatically generated atlases. (Table 1, Hand-Drawn)
Participant Macroanatomical Atlas
Automatic creation of macroanatomical atlas based on Hammers and LPBA40 atlases, using the Gousias et al (2008) method of registration and majority vote. Done for all MCBI participants making up the average MRI templates, and all NIHPD participants at ages 3, 6, 9, and 12 months. Linear: linear registration of the segmented adult atlases to the individual infant participants. Non-linear: non-linear registration of the segmented adult atlases to individual infant participants. These atlases represent an approach to construct a macroanatomical atlas for individual infant participants. (Table 1, Majority Vote).
Average Template Macroanatomical Atlases
Automatic creation of macroanatomical atlas based on Hammers and LPBA40 atlases. Based on majority vote procedure with individual MCBI participant macroanatomical atlases making up the average MRI templates. Done at 3, 4.5 6, 7.5, 9, and 12 months. Linear: linear registration of the linear-constructed participant macroanatomical atlas to the average MRI template. Non-linear: nonlinear registration of the nonlinear-constructed participant macroanatomical atlas to the average MRI template. This is an average atlas that may be used for automatic atlas registration / transformation to individual participants (Table 1, Automatic-Average)

Table 3

Steps for delineation of manual atlas.

1. Mask the insula and non-cortical areas. Non-cortical areas include cerebellum, brainstem, thalamus, corpus callosum, and striatum (putamen, caudate). Use the protocols developed for the LONI LPBA40 atlas. http://resource.loni.usc.edu/resources/downloads/research-protocols/probalistic-atlas/cerebellum/ http://resource.loni.usc.edu/resources/downloads/research-protocols/probalistic-atlas/brainstem/ http://resource.loni.usc.edu/resources/downloads/research-protocols/masking-regions/thalamus/ http://resource.loni.usc.edu/resources/downloads/research-protocols/segmentation/caudate-delineation/ http://resource.loni.usc.edu/resources/downloads/research-protocols/masking-regions/insular-cortex/
2. Identify the ventricles using an average T2W MRI. Thresholding the CSF by using the values found in the internal ventricles; use this threshold to identify CSF in ventricles throughout brain.
3. Mask the frontal and temporal lobes. Use the LONI protocols to identify the areas for either frontal or temporal lobes. http://resource.loni.usc.edu/resources/downloads/research-protocols/masking-regions/frontal-lobe-left/ Temporal: http://resource.loni.usc.edu/resources/downloads/research-protocols/probalistic-atlas/inferior-temporal-gyrus/ http://resource.loni.usc.edu/resources/downloads/research-protocols/probalistic-atlas/parahippocampal-gyrus/ http://resource.loni.usc.edu/resources/downloads/research-protocols/probalistic-atlas/middle-temporal-gryus/ http://resource.loni.usc.edu/resources/downloads/research-protocols/masking-regions/middle-temporal-gyrus/ http://resource.loni.usc.edu/resources/downloads/research-protocols/masking-regions/superior-temporal-gyrus/ http://resource.loni.usc.edu/resources/downloads/research-protocols/probalistic-atlas/superior-temporal-gyrus/
4. Mask the occipital area. For occipital area, use the MNI Structural Atlas definition (Mazziotta, Toga et al. 2001) provided with FSL. A first approximation was generated by registering the infant average template to the 20-24 year template, and transforming the lobar atlas from the 20-24 year template to the infant average template. The areas were then manually adjusted for the infant atlas.
5. Mask the cortical sub-lobar areas (fusiform, cingulate). The definition from the FSL Harvard-Oxford Atlases (Desikan, Segonne et al. 2006) and the LONI protocols were used. A first approximation was generated by registering the infant average template to the 20-24 year template, and transforming the lobar atlas from the 20-24 year template to the infant average template. These areas were manually adjusted to match the areas for the infant atlas, and adjusted to match the areas in the LONI segmenting protocols. http://resource.loni.usc.edu/resources/downloads/research-protocols/probalistic-atlas/fusiform-gyrus/ http://resource.loni.usc.edu/resources/downloads/research-protocols/probalistic-atlas/cingulate-gyrus/
6. Mask the parietal lobe. The parietal lobe was the brain area in the parietal area left after the surrounding areas were identified (e.g., occipital, frontal, temporal) and was manually adjusted to match the separate areas in the LONI segmenting protocols. http://resource.loni.usc.edu/resources/downloads/research-protocols/masking-regions/parietal-lobe/
7. The resulting areas were put in a single MRI volume, with the sub-lobar areas (cingulate, fusiform gyrus) masking out the corresponding voxels from the lobar areas. All 14 areas were retained in separate MRI volumes.

Table 4

Overlap between the areas of the manual atlas and the LPBA40 atlas, and the manual atlas and the Hammers atlas. Numbers are the segment numbers on the atlas. % Overlap is the shared overlap between the Manual Atlas and the other atlases averaged across the 6 infant ages.

Manual Atlas Label	Hammers Atlases Label	% Overlap	LPBA40 Atlas Label	% Overlap
1. Other				
2.Ventricles	45-46. Lateral ventricle, frontal horn, central part and occipital horn (left, right)	44, 43		
	49. Third ventricle	46		
3. Cerebellum	17-18. Cerebellum (left, right)	86, 86	181. Cerebellum	92
4. Brainstem	19. Brainstem	85	182. Brainstem	93
	74-75. Substantia Nigra (left, right)	98, 97		
5. Thalamus	40-41. Thalamus (left, right)	62, 65		
6. Striatum	34-35. Caudate nucleus (left, right)	57, 57	161-162. Caudate (left, right)	44,42
	36-37. Nucleus accumbens (left, right)	68, 78		
	38-39. Putamen (left, right)	78, 81	163-164. Putamen (left, right)	69, 71
	42-43. Globus pallidus (left, right)	46, 42		
7. Corpus Callosum	44. Corpus Callosum	60		
8. Cingulate	24-25. Cingulate gyrus, anterior part (left, right)	90, 91	121-122. Cingulate gyrus (left, right)	72, 78
	26-27. Cingulate gyrus, posterior part (left, right)	88, 91		
	76-77. Subgenual frontal cortex (left, right)	78, 80		
	78-79. Subcallosal area (left, right)	73, 49		
	80-81. Pre-subgenual frontal cortex (left, right)	72, 90		
	52-53. Straight gyrus (left, right)	33, 30		
9. Insula	20-21. Insula (left, right)	48, 51	101-102. Insular cortex (left, right)	67, 71
10. Frontal	28-29. Middle frontal gyrus (left, right)	81, 84	23-24. Middle frontal gyrus (left, right)	81, 82
	50-51. Precentral gyrus (left, right)	61, 64	27-28. Precentral gyrus (left, right)	55,55
	52-53. Straight gyrus (left, right)	58, 61	33-34. Straight gyrus (left, right)	64, 65
	54-55. Anterior orbital gyrus (left, right)	89, 90		
	56-57. Inferior frontal gyrus (left, right)	84, 85	25-26. Inferior frontal gyrus (left, right)	79, 82
	58-59. Superior frontal gyrus (left, right)	80, 79	21-22. Superior frontal gyrus (left, right)	72, 72
	68-69. Medial orbital gyrus (left, right)	91, 91	29-30. Middle orbitofrontal gyrus (left, right)	88, 88
	70-71. Lateral orbital gyrus (left, right)	84, 83	31-32. Lateral orbitofrontal gyrus (left, right)	78, 76
	72-73. Posterior orbital gyrus (left, right)	88, 88		

Manual Atlas Label	Hammers Atlases Label	% Overlap	LPBA40 Atlas Label	% Overlap
11. Occipital	22-23. Lateral remainder of occipital lobe (left, right)	43, 45	61-62. Superior occipital gyrus (left, right)	68, 68
			63-64. Middle occipital gyrus (left, right)	42, 37
			65-66. Inferior occipital gyrus (left, right)	33, 0
	64-65. Lingual gyrus (left, right)	48, 39	89-90. Lingual gyrus (left, right)	39, 40
	66-67. Cuneus (left, right)	95, 95	67-68. Cuneus (left, right)	89, 95
12. Fusiform	15-16. Lateral occipitotemporal gyrus (left, right)	68, 81	91-92. Fusiform gyrus (left, right)	59, 68
	9-10. Parahippocampal gyrus (left,right)	37, 39	87-88. Parahippocampal gyrus (left, right)	41, 45
	64-65. Lingual gyrus (left, right)	55, 53	89-90. Lingual gyrus (left, right)	52, 51
13. Temporal	1-2. Hippocampus (left, right)	64, 75	165-166. Hippocampus (left, right)	64, 74
	3-4. Amygdala (left, right)	86, 89		
	5-6. Anterior temporal lobe medial part (left, right)	73, 77		
	7-8. Anterior temporal lobe lateral part (left, right)	73, 78	83-84. Middle temporal gyrus (left, right)	71, 80
	9-10. Parahippocampal gyrus (left, right)	50, 54		
	11-12. Superior temporal gyrus, central (left, right)	92, 94	81-82. Superior temporal gyrus (left, right)	72, 81
	82-83. Superior temporal gyrus, anterior part (left, right)	84, 85		
	13-14. Medial and inferior temporal gyri (left, right)	85, 85	85-86. Inferior temporal gyrus (left, right)	64, 67
	30-31. Posterior temporal lobe (left, right)	45, 54		
14. Parietal	60-61. Postcentral gyrus (left, right)	80,78	41-42. Postcentral gyrus (left, right)	84, 85
	62-63. Superior parietal gyrus (left, right)	81, 80	43-44. Superior parietal gyrus (left, right)	84, 84
	32-33. Remainder of the parietal lobe (left, right)	89, 91	45-46. Supramarginal gyrus (left, right)	82, 88
	22-23. Lateral remainder of occipital lobe (left, right)	45, 45	47-48. Angular gyrus (left, right)	86, 85
			49-50. Precuneus (left, right)	80,77
			63-64. Middle occipital gyrus (left, right)	46, 45
			65-66. Inferior occipital gyrus (left, right)	22, 35

Table 5

Comparisons between atlas approaches examined in the current study.

1. Manually delineated regions versus registration/transformation to template atlas Overlap between manually delineated regions and regions resulting from linear/non-linear registration/transformation to the age-appropriate template-based atlas, and older age template-based atlases. The Dice coefficient (Dice, 1945; Crum et al., 2005) was used to evaluate the overlap of MRI atlas volumes. The Dice coefficient measures degree of overlap (ranging from 0 [no overlap] to 1 [total overlap]), and represents the intersection of two similarly labeled regions divided by the mean volume of the regions. We also calculated the 'target overlap' (Crum et al., 2005). This represents the sensitivity of the analysis, and is a measure of segment concordance when there are some areas in the reference segment not fully represented in the target segment.	MCBI and NIHPD: Four at 3, 6, 9, 12 months Two at 4.5 and 7.5 months
2. Manually delineated regions versus individual macroanatomical atlas and versus age-based template transformed atlas. Overlap between manually delineated regions and regions resulting from the majority vote approach to individual macroanatomical atlas creation, or regions coming from age-appropriate average atlas with linear / non-linear registration/transformation to participant space	MCBI and NIHPD: Four at 3, 6, 9, 12 months Two at 4.5 and 7.5 months Internal:MCBI
3. Individual macroanatomical atlases vs registration/transformation to average macroanatomical atlas Overlap between regions resulting from the majority vote approach to individual macroanatomical atlas creation and linear/non-linear registration/transformation of an age-based atlas into the participant space..	N=14, 12, 14, 11, 8, 10 at 3, 4.5, 6.0, 7.5, 9, 12 months External: NIH N = 20, 32, 28, and 25 at 3, 6, 9, 12 months